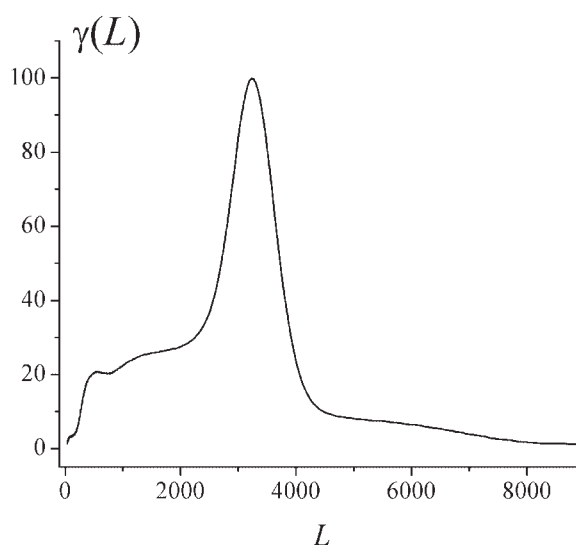


# Determination of the Mode of Free Radical Termination from Pulsed Laser Polymerization Experiments

Anatoly N. Nikitin, Robin A. Hutchinson\*

The molecular-weight distribution (MWD), obtained by pulsed laser polymerization (PLP) at the high termination rate limit has been considered for investigating termination kinetics. The proposed methodology takes into account both the composite model for termination and the chain-length dependence of propagation for short-chain and long-chain radicals. Power-law expressions are used to represent propagation [ $k_p^L = k_p^0(L)^{-\alpha}$ ] and termination [ $k_t^{L,L} = k_t^0(L)^{-\beta}$ ] of long-chain radicals (where  $k_p^0$  and  $k_t^0$  represent the maximum “virtual” rate coefficients for monomeric radicals, and  $\alpha$  and  $\beta$  capture the chain-length dependencies for propagation and termination), with the combined value of  $(\beta - \alpha)$  evaluated from the MWD, after correcting for the influence of the kinetics of short-chain radicals. A novel method is also developed for determining the mode of termination,  $\delta$ , from MWDs produced by PLP at the high termination rate limit. Simulations for methyl methacrylate (MMA) polymerization at 25 °C confirm that the method can be applied robustly in the presence of complicating factors such as chain transfer to monomer and SEC broadening. The analysis of an experimental MWD obtained for MMA polymerization at 25 °C results in estimates of  $0.14 \pm 0.03$  for  $(\beta - \alpha)$  and  $0.75 \pm 0.04$  for  $\delta$ .



## Introduction

Pulsed laser polymerization (PLP) techniques, first introduced in the late 1980s, continue to provide valuable insights into propagation and termination kinetics of free radical polymerization systems. While different variants exist, they are all based on the almost instantaneous generation of radicals by application of a UV laser pulse to a monomer solution containing photoinitiator. The group

A. N. Nikitin  
Institute on Laser and Information Technologies, Svyatoozerskaya  
1, Shatura, Moscow Region 140700, Russia  
R. A. Hutchinson  
Department of Chemical Engineering, Dupuis Hall, Queen's  
University, Kingston, Ontario, Canada K7L 3N6  
Fax: (+1) 613 533 6637; E-mail: robin.hutchinson@chee.queensu.ca

of Buback combines PLP with near-infrared spectroscopy to measure monomer consumption resulting from the application of a single pulse,<sup>[1]</sup> analyzing the rate data to determine termination kinetics as a function of monomer conversion, chain length, and (for copolymerization) monomer composition.<sup>[2]</sup> However, as a rate-based method, the technique cannot be used to determine if the mutual termination of propagating radicals  $R_i\cdot$  (where  $i$  is the number of monomer units) in free-radical polymerization occurs via combination



or disproportionation



where  $P_i$  is a dead macromolecule with chain length  $i$ , and  $k_{tc}$  and  $k_{td}$  are the rate coefficients of termination by combination and disproportionation, respectively. The proportion of combination and disproportionation termination reactions depends upon the type of monomer being polymerized. The temperature is also found to influence this proportion.<sup>[3–6]</sup> As the mode of termination can have a marked effect on many aspects of polymer properties, it has been a long-standing subject of investigation.<sup>[3–11]</sup> The mode of termination affects the shape of the molecular-weight distribution (MWD), therefore an accurate knowledge of the distribution could allow the relative proportion of the termination reactions to be assessed.<sup>[5,6]</sup> Analysis of MWDs and other experimental approaches have been developed to determine the mode of termination,<sup>[5–8]</sup> but accurate values are difficult to obtain even for such monomers as methyl methacrylate (MMA) and styrene,<sup>[9]</sup> many estimates are based largely on theoretical considerations.<sup>[6,10,11]</sup>

Analysis of polymer MWD is the basis of the standard PLP technique used mainly to study propagation kinetics. For this technique, a mixture of monomer and photoinitiator is illuminated by laser pulses separated by a time of  $t_0$ , typically 0.01–0.2 s. Each pulse generates a burst of new radicals in the reaction mixture that will grow, provided that they escape termination, to a chain length  $L_0$ .<sup>[12,13]</sup>

$$L_0 = k_p[M]t_0 \quad (2)$$

with  $[M]$  the monomer concentration and  $k_p$  the propagation rate coefficient. There is a high probability that the new radicals from the subsequent flash at  $t_0$  will terminate these chains, such that a distinctive peak is formed in the polymer MWD corresponding to  $L_0$ . The position of  $L_0$ , usually determined from the inflection point

of the MWD, is not sensitive to the mode of termination, as the reaction is between a very short radical and a radical of length  $L_0$ .<sup>[12]</sup> Since radicals have a certain probability to survive the burst of termination at  $t_0$  and to terminate at a later pulse, the relative concentration of polymer with chain lengths  $2L_0, 3L_0, \dots$  is also increased. As a result, the technique produces a well-structured MWD with peaks at chain length of  $L_0$  and its multiples. The relative magnitude of these peaks as well as the shape of the entire distribution depends on the mode of termination, as well as on the fraction of radicals terminated between two successive laser pulses,  $\gamma_t$ . Neglecting chain-length dependence of rate coefficients and using the IUPAC recommended<sup>[14]</sup> convention for the rate of loss of free radicals by termination ( $-2k_tR^2$ ), this latter quantity is written as<sup>[15]</sup>

$$\gamma_t = \frac{2k_tR_0t_0}{1 + 2k_tR_0t_0} \quad (3)$$

where  $R_0$  is the radical concentration generated per pulse. For a given system,  $\gamma_t$  can be increased by increasing  $R_0$  (controlled largely by photoinitiator concentration and laser power) or the time between pulses. In the so-called “high termination rate limit”,<sup>[16]</sup> almost all of the polymer chains formed are terminated before the next pulse arrives ( $\gamma_t$  approaches unity) such that the secondary features of the MWD controlled by  $k_p$  are lost.<sup>[15]</sup> These conditions, however, are useful for studying the mode of termination, as described below.

The PLP-MWD technique has been applied to measure  $k_p$  for many monomers of industrial significance over a range of temperatures, with good agreement (generally within 15%) achieved between facilities around the world;<sup>[2,17,18]</sup> a modified version of the technique has also been used to evaluate chain transfer constants.<sup>[19–21]</sup> In recent years, it has been proposed that some of the minor discrepancies reported in  $k_p$  values arise from a chain-length dependence, with monomer addition to short radicals significantly faster than addition to long-chain radicals,<sup>[6,22–31]</sup> the possible influence of both chain-length dependent propagation and termination will be considered further in this work.

Olaj and Schnöll-Bitar<sup>[13]</sup> were the first to utilize MWDs obtained by PLP for determining the mode of termination. The weight distribution  $[m(L) = Ln(L)]$ , where  $n(L)$  is the number distribution] was examined in three regions:  $0 < L \leq L_0$ ,  $L_0 < L \leq 2L_0$  and  $2L_0 < L \leq 3L_0$ . Analytical expressions for the relative heights of the distributions at specified points in the three regions were derived to evaluate the mode of termination. PLP-generated MWDs were used to estimate the relative contribution of disproportionation to total termination,  $\delta$ , as essentially zero for

styrene and 0.1 for MMA at 25 °C. Based on the latter result, the authors conclude that the methodology does not provide a reliable estimate for  $\delta$ . Evseev and Nikitin<sup>[32]</sup> suggested a variation of this method, using only two intervals  $0 < L \leq L_0$  and  $L_0 < L \leq 2L_0$  from the PLP-generated MWD, and using the weight-log distribution  $[w(\log_{10} L) = L^2 n(L)]$  directly as measured by size-exclusion chromatography (SEC); however they did not check their proposal experimentally. Sarnecki and Schweer<sup>[16]</sup> were the first to suggest that the mode of termination could be more easily determined at the PLP high termination rate limit: there is a marked shoulder for termination by combination ( $\delta = 0$ ) at the right side of distribution from the PLP peak, while this shoulder is absent for the case of termination by disproportionation ( $\delta = 1$ ). They qualitatively concluded that both styrene and MMA are terminated predominantly by combination at 25 °C. The finding for MMA is contrary to most of the literature,<sup>[6–11]</sup> suggesting that the high termination rate limit was not achieved by their PLP experimental conditions. Nikitin<sup>[33]</sup> derived analytical expressions to quantitatively determine  $\delta$  at the high termination rate limit, also taking into account the chain-length dependence of termination.

These previous efforts indicate that there is still a need to develop a robust methodology to estimate the mode of termination from PLP-MWD experiments. In this work, a new procedure is proposed for PLP conducted at the high termination rate limit, considering the chain-length dependence of both propagation and termination. In addition, the PLP-generated MWDs are analyzed to estimate the power-law exponent describing these combined chain-length dependencies. Extensive simulations are carried out to confirm that the methods can be successfully applied under the influence of complicating factors (chain transfer to monomer, SEC broadening, etc.), using MMA polymerization at 25 °C as an example. An experimental MWD obtained by PLP of MMA at the high termination rate limit has been analyzed to determine the mode of termination.

## Method Development

At the high termination rate limit, the shape of the MWD is largely controlled by propagation and termination kinetics of radicals formed by a single pulse, not a sequence of pulses. According to recent publications,<sup>[24,30,31,34]</sup> both mechanisms should be considered to be chain-length dependent for correct treatment of experimental data. Therefore, the chain-length dependence for both reactions are taken into account in the expression derived for  $n_s(L)$ , the concentration of macromolecules of chain length  $L$

formed from a single laser pulse in the absence of chain transfer events<sup>[33,35]</sup>

$$n_s(L) = \frac{2R_0^2 k_{td}^{L,L}}{[M]k_p^L \left( 1 + 2R_0 \int_0^{\varphi(L)} k_t^{\psi(t'), \psi(t')} dt' \right)^2} + \frac{R_0^2 k_{tc}^{L/2, L/2}}{2[M]k_p^{L/2} \left( 1 + 2R_0 \int_0^{\varphi(L/2)} k_t^{\psi(t'), \psi(t')} dt' \right)^2} \quad (4)$$

In Equation (4),  $R_0$  is the radical concentration produced by the single pulse,  $[M]$  is the monomer concentration,  $k_{tc}^{L,L}$  and  $k_{td}^{L,L}$  are the termination rate coefficients of radicals with chain length  $L$  by combination and disproportionation, respectively ( $k_t^{L,L} = k_{tc}^{L,L} + k_{td}^{L,L}$ ); as all radicals are generated at the same instant in time, it is only necessary to consider termination between radicals of the same length.  $k_p^L$  is the propagation rate coefficient of radicals with chain length  $L$ ,  $\psi(t)$  is the solution of the equation

$$\frac{dL}{dt} = k_p^L [M] \quad (5)$$

and  $\varphi(L)$  is the inverse function to  $L = \psi(t)$ . In deriving Equation (4), the rate of loss of free radicals by termination is chosen to be  $-2k_t^{L,L} R^2$  as recommended by IUPAC.<sup>[14]</sup>

To proceed further, it is necessary to assume a functional form to describe how propagation and termination rate coefficients vary with chain length. Above some critical chain length  $L_f$ , both the propagation and termination are represented by power-law expressions

$$k_p^L = k_p^0 (L)^{-\alpha} \quad (6a)$$

$$k_t^{L,L} = k_t^0 (L)^{-\beta} \quad (6b)$$

where  $k_p^0$  and  $k_t^0$  represent the maximum virtual rate coefficient for monomeric radicals, and  $\alpha$  and  $\beta$  capture the chain-length dependence for propagation and termination of chain lengths above  $L_f$ . Equation (6) does not take into account that the dependence on chain length is often stronger for chains shorter than  $L_f$ . For example, according to the composite model proposed recently by Smith et al.,<sup>[36]</sup> the termination rate coefficients  $k_t^{L,L}$  can be expressed as

$$k_t^{L,L} = k_t^{1,1} L^{-e_1}, \quad L \leq L_t \quad (7a)$$

$$k_t^{L,L} = k_t^{1,1} L_f^{(-e_1 + \beta)} L^{-\beta}, \quad L \geq L_t \quad (7b)$$

In this expression,  $L_t$  represents the chain length separating macromolecules with termination rate controlled by

center-of-mass diffusion ( $L \leq L_t$ ) from those for which segmental reorientation controls rate ( $L \geq L_t$ ). Equation (6b) and (7b) are equal with  $L_t = L_f$  and  $k_t^0 = k_t^{1,1} L_f^{(-e_1 + \beta)}$ .

It is also known that the first few addition steps to a newly formed radical occur at a faster rate than monomer addition to long-chain radicals.<sup>[6]</sup> In the previous work,  $k_p^L$  was subdivided into two regions with different power-law exponents,<sup>[23]</sup> as shown for termination above. However, more recently the following expression has been suggested to provide a physically realistic description for propagation of short chains<sup>[31,34]</sup>

$$k_p^L = k_p \left[ 1 + C_1 \exp\left(\frac{-\ln 2}{i_{1/2}}(L - 1)\right) \right], \quad L \leq L_c \quad (8)$$

where  $C_1 = (k_p^1 - k_p)/k_p$  and  $i_{1/2}$  are parameters that dictate the chain-length dependence of  $k_p^L$ ,  $k_p$  is the constant value for propagation of long chains, and  $L_c$  is the chain length separating the two regions with the different chain-length dependent laws. This expression is combined with the power-law relationship [Equation (6a)] describing propagation in the long-chain region, as detailed in Appendix B. Although this power-law representation has some limitations ( $k_p^L$  approaches zero for infinite chain length), it simplifies considerably the theoretical consideration of MWDs. Furthermore, the chain-length dependence is very weak ( $\alpha \approx 0.07$ )<sup>[26]</sup> such that calculated values never approach zero for the range of chain lengths considered in this work (e.g.;  $k_p$  ( $L \cdot \text{mol}^{-1} \cdot \text{s}^{-1}$ ) decreases from 303 at  $L = 10^3$  to 258 at  $L = 10^4$ ), and it has been shown that the application of this law results in very similar predictions as the ones obtained by using other models.<sup>[25]</sup> Note that  $L_c < L_t$ ,<sup>[30,31]</sup> therefore, in the following consideration  $L_f$  is chosen to be  $L_t$ .

Substituting the power-law relationships [Equation (6)] into Equation (4) yields for  $L \geq L_f$

$$n_s(L) = \frac{2\delta k_t^0 R_0^2 L^{\alpha-\beta}}{U \left( 1 + 2R_0 \frac{k_t^0 L^{1+\alpha-\beta} p(L)}{(1+\alpha-\beta)U} \right)^2} + \frac{(1-\delta)k_t^0 R_0^2 L^{\alpha-\beta}}{2^{1+\alpha-\beta} U \left( 1 + R_0 \frac{k_t^0 L^{1+\alpha-\beta} d(L)}{2^{\alpha-\beta}(1+\alpha-\beta)U} \right)^2} \quad (9)$$

where  $U = k_p^0 [M]$ ,

$$p(L) = 1 + \frac{\frac{(1+\alpha-\beta)U}{k_t^0} b - L_f^{1+\alpha-\beta}}{L^{1+\alpha-\beta}} \quad (10a)$$

$$d(L) = 1 + \frac{\frac{(1+\alpha-\beta)U}{k_t^0} b - L_f^{1+\alpha-\beta}}{(L/2)^{1+\alpha-\beta}} \quad (10b)$$

$$b = \int_0^{\varphi(L_f)} k_t^{\psi(t'), \psi(t')} dt' \quad (10c)$$

If we assume that Equation (6) is valid for the entire chain-length domain  $0 \leq L < \infty$  ( $L_f = 0$ ), then the chain length distribution  $n_s(L)$  is described by Equation (9) with  $p(L) = 1$  and  $d(L) = 1$ . Thus, the functions  $p(L)$  and  $d(L)$  can be considered as correction factors accounting for the different propagation and termination behavior of very short chains. The two functions are related by  $d(L) = 1 + 2^{1+\alpha-\beta}[p(L) - 1]$ . For the special case when  $k_p$  is assumed to be chain-length independent, and the chain-length dependence of termination is described by Equation (6b) over the entire chain-length domain ( $L_f = 0$ ), Equation (9) reduces to

$$n_s(L) = \frac{2\delta k_t^0 R_0^2 L^{-\beta}}{U \left( 1 + 2R_0 \frac{k_t^0 L^{1-\beta}}{(1-\beta)U} \right)^2} + \frac{(1-\delta)k_t^0 R_0^2 L^{-\beta}}{2^{1-\beta} U \left( 1 + 2R_0 \frac{k_t^0 L^{1-\beta}}{2^{1-\beta}(1-\beta)U} \right)^2} \quad (11)$$

This equation, first published by Nikitin and Evseev,<sup>[37]</sup> led to the proposal for investigating chain-length dependent termination (determining the exponent  $\beta$ ) by polymerization with packets of closely spaced laser pulses followed by a long dark period<sup>[35,37]</sup> as well as for PLP at the high termination rate limit.<sup>[33]</sup> Later Olaj et al.<sup>[38]</sup> rederived Equation (11) in normalized form for estimating  $\beta$  in the low frequency (high termination rate) limit of polymerization. Equation (9) extends these efforts by introducing chain-length dependent propagation, and the functions  $p(L)$  and  $d(L)$  to correct for the different polymerization behavior of short chains.

## A Novel Method for Determination of the Mode of Termination

Sarnecki and Schweer<sup>[16]</sup> first reported that for PLP performed at the high termination rate limit, a shoulder on the high MW side of the PLP-generated MWD peak is associated with the mode of termination. However, their qualitative approach was based on analysis of the MWD on a weight-fraction basis [ $m(L)$  proportional to  $\ln(L)$ ], rather than the weight-log form  $w(\log_{10} L)$ . This latter form, proportional to  $L^2 n(L)$ , comes directly from SEC when a mass sensitive detector is used. MWDs in  $w(\log M)$  form, calculated at the PLP high termination rate limit for MMA

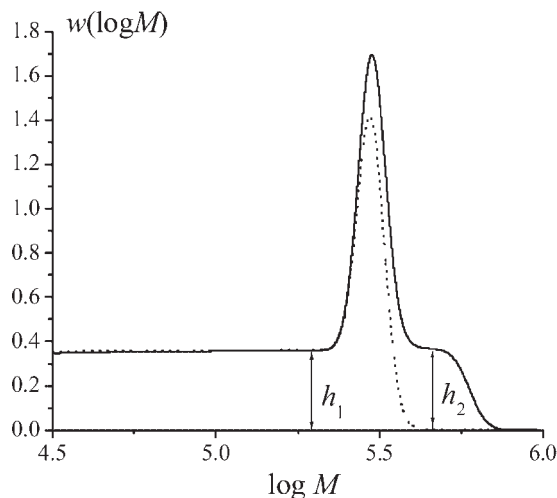


**Figure 1.** MWDs calculated for PLP at the high termination rate limit for MMA at 25 °C with termination exclusively by combination (solid line) and exclusively by disproportionation (dashed line). The kinetic parameters used for the simulation are assumed to be chain length-independent, with  $[M] = 9.354 \text{ mol} \cdot \text{L}^{-1}$ ,  $k_t = 4.1 \times 10^7 \text{ L} \cdot \text{mol}^{-1} \cdot \text{s}^{-1}$ ,  $k_p = 318 \text{ L} \cdot \text{mol}^{-1} \cdot \text{s}^{-1}$ ,  $\sigma_v b = 0.04$ ,  $t_0 = 1 \text{ s}$ , and  $R_0 = 10^{-5} \text{ mol} \cdot \text{L}^{-1}$ .

at 25 °C are presented in Figure 1 for the cases of termination by combination (solid line) and disproportionation (dotted line). These distributions are calculated using a classical model, neglecting chain transfer, and chain-length dependencies of propagation and termination, to compare with the distributions from ref.<sup>[16]</sup> given in  $m(L)$  form. The analytical expressions derived in ref.<sup>[39]</sup> have been used for the calculation, with  $k_p = 318 \text{ L} \cdot \text{mol}^{-1} \cdot \text{s}^{-1}$ <sup>[40]</sup> and  $k_t = 4.1 \times 10^7 \text{ L} \cdot \text{mol}^{-1} \cdot \text{s}^{-1}$ .<sup>[2]</sup> The effect of SEC instrument broadening on the MWD has been introduced in accordance with ref.<sup>[41]</sup> with the parameter  $\sigma_v b = 0.04$ . The pulse separation time and the initial radical concentration are chosen to be  $t_0 = 1 \text{ s}$  and  $R_0 = 10^{-5} \text{ mol} \cdot \text{L}^{-1}$ . The high MW shoulder for the case where termination occurs exclusively by combination is much more pronounced for the  $w(\log_{10} L)$  distributions than the one for the  $m(L)$  distributions from ref.<sup>[16]</sup> In addition, the ordinates of the  $w(\log_{10} L)$  distribution immediately before and after the peak are very close to each other:  $h_1 \approx h_2$  in Figure 1. The attempt to explain this circumstance has led to the new method for determination of  $\delta$  developed below.

The reason for the low MW shoulder of the PLP peak produced at the high termination rate limit has been explained in ref.<sup>[16,33]</sup> and is also presented in Appendix A. This portion of the distribution is controlled by propagation and termination events that occur before the next pulse arrives, as found for a single pulse [Equation (4)]. Reintroducing chain-length dependent propagation and

termination, the weight-log distribution on the low MW side of the peak is described by

$$\gamma_{\text{left}}(L) = a_p n_s(L) L^2 = \frac{a_p (1 + \alpha - \beta)^2 U L^{\beta - \alpha}}{2 k_t^0} \times \left( \frac{\delta}{p(L)^2} + \frac{(1 - \delta) 2^{\alpha - \beta}}{d(L)^2} \right) \quad (12)$$

where  $a_p$  is a proportionality factor. A plot of  $\ln(\gamma_{\text{left}}(L))$  versus  $\ln L$  can be used to study chain-length dependent kinetics. In the absence of chain-length dependent propagation, and assuming a single power-law relationship for termination [ $L_f = 0$  for Equation (6b)], the slope yields the exponent  $\beta$ .<sup>[33,35]</sup> Under the more complex kinetics considered here, the slope of the log-log plot is  $(\beta - \alpha + \alpha_{\text{add}})$ , where  $\alpha$  is the chain-length dependence of long chain propagation [Equation (6a)] and  $\alpha_{\text{add}}$  is a new term introduced to capture the stronger effect of chain-length propagation and termination dependencies observed for short chains

$$\ln(\gamma_{\text{left}}(L)) = \ln(B) + (\beta - \alpha + \alpha_{\text{add}}) \ln(L) \quad (13)$$

The intercept  $B = [a_p (1 + \alpha - \beta)^2 U / 2 k_t^0] g$  is a constant that is independent of chain length, and  $g$  and  $\alpha_{\text{add}}$  are parameters arising from the  $p(L)$  and  $d(L)$  functions defined by Equation (10)

$$g L^{\alpha_{\text{add}}} = \frac{\delta}{p(L)^2} + \frac{(1 - \delta) 2^{\alpha - \beta}}{d(L)^2} \quad (14)$$

Equation (12)–(14) are an extension of the method outlined in ref.<sup>[33]</sup> for estimating chain-length dependencies from MWDs obtained by PLP at the high termination rate limit. The slope, however, is a function not only of chain-length dependent termination, but is also affected by chain-length dependent propagation kinetics and the extent of the stronger dependencies occurring for short chains.

Later, we will consider how the value of  $\alpha_{\text{add}}$  can be estimated. Before doing so, however, we return to the PLP-generated MWD obtained at the high termination rate limit, this time considering the distribution on the right side of the peak. As discussed more fully in Appendix A, at the high termination rate limit the chains in this region are formed exclusively due to termination by combination, expressed as

$$\gamma_{\text{right}}(L) = a_p (n_s(L) L^2)_{\text{combination}} = \frac{a_p (1 + \alpha - \beta)^2 U L^{\beta - \alpha} (1 - \delta) 2^{\alpha - \beta - 1}}{k_t^0 d(L)^2} \quad (15)$$



As shown in Figure 1, the ordinates  $h_1$  and  $h_2$  are measured at chain lengths  $L_1$  and  $L_2$  from the left and right sides of the MWD peak:  $h_1 = \gamma_{\text{left}}(L_1)$  and  $h_2 = \gamma_{\text{right}}(L_2)$ . Defining the ratio  $\omega_h = h_2/h_1$ , the following expression is derived to determine the fraction of termination by disproportionation  $\delta$

$$\delta = \frac{1}{1 + \frac{2^{\beta-\alpha} \omega_h}{\left(\frac{L_2}{L_1}\right)^{\beta-\alpha} \left(\frac{p(L_1)}{d(L_2)}\right)^2 - \omega_h \left(\frac{p(L_1)}{d(L_1)}\right)^2}} \quad (16a)$$

For the classical model of free radical polymerization (neither propagation nor termination are chain-length dependent) Equation (16a) simplifies to

$$\delta = 1 - \omega_h \quad (16b)$$

Equation (16) is the basis of the proposed method to determine the mode of termination.

The following steps, illustrated in Figure 2, are required to estimate  $\delta$

- Transform the PLP-generated MWD obtained at the high termination rate limit from the  $w(\log_{10} M)$  form to  $\gamma(L) = a_p n(L) L^2$  by plotting  $w(\log_{10} M)$  against  $L$  instead of versus  $\log_{10} M$ .
- Plot the distribution as  $\ln[\gamma(L)]$  versus  $\ln L$  and evaluate  $(\beta - \alpha + \alpha_{\text{add}})$  by linear regression of points in the vicinity of the peak on the low MW side. This region is a plateau if there are no chain-length dependencies, but otherwise has observable slope. The end point of the region is chosen at a position immediately before the start of the sharp rise of the main peak of the MWD, and the initial point is selected to provide a reasonable estimate for the slope while remaining well above  $L_f$ . To determine  $(\beta - \alpha)$ , the value of  $\alpha_{\text{add}}$  must be estimated from the current knowledge of  $p(L)$  and  $d(L)$  functions for the monomer system of interest, as discussed below.
- Evaluate  $h_1$  and  $h_2$  from the distribution, with  $h_1$  chosen from the region of the distribution used for linear regression in (b). It is recommended that  $h_2$  be evaluated at chain length  $L_{2\text{max}}$ , corresponding to the maximum of the second peak of the derivative plot obtained by differentiating the  $\gamma(L)$  distribution, such that  $h_2 = \gamma(L_{2\text{max}})$ .
- Apply Equation (16) to determine the value of  $\delta$ .

Further justification of this method is provided and checked by simulation, before it is applied to determine kinetic parameters from an experimental MWD obtained from PLP of MMA at the high termination rate limit.

## Support of the Method by Simulation

To examine the robustness of the method, it is necessary to check the extent to which complicating factors might affect its application. Using MMA as an example, the following factors are examined: (a) chain transfer to monomer, (b) SEC broadening, and (c) the role of  $p(L)$  and  $d(L)$  functions on the chain-length regions chosen when applying the method. Also, the conditions required to work at the high termination rate limit are carefully checked.

The first factor, chain transfer to monomer, is taken into account in all simulations by using the analytical expressions derived in ref.<sup>[39]</sup> to calculate MWDs. With a chain transfer constant ( $C_M$ ) of  $10^{-5}$ ,<sup>[42]</sup> the mechanism has negligible effect on the shape of the MWD produced by PLP at the high termination rate limit if the laser pulse repetition rate is higher than or equal to 1 Hz.

## Influence of SEC Broadening

The importance of SEC broadening becomes clear from Figure 3, in which the same distribution is presented for

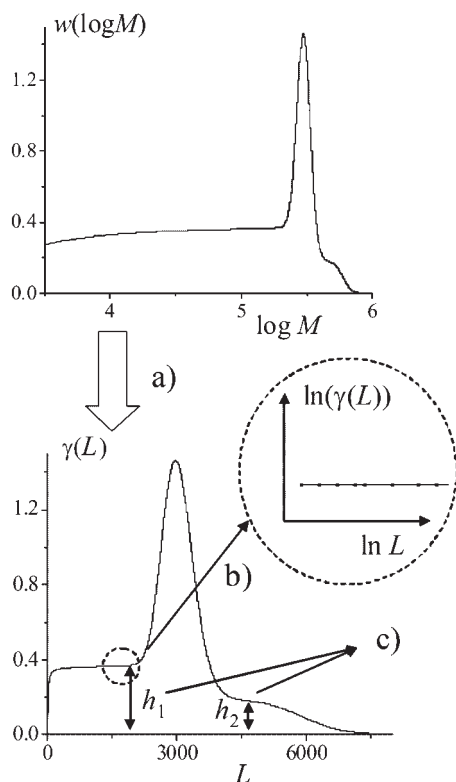


**Figure 2.** Steps towards determining the mode of termination. The example MWD is calculated assuming no chain-length dependencies.

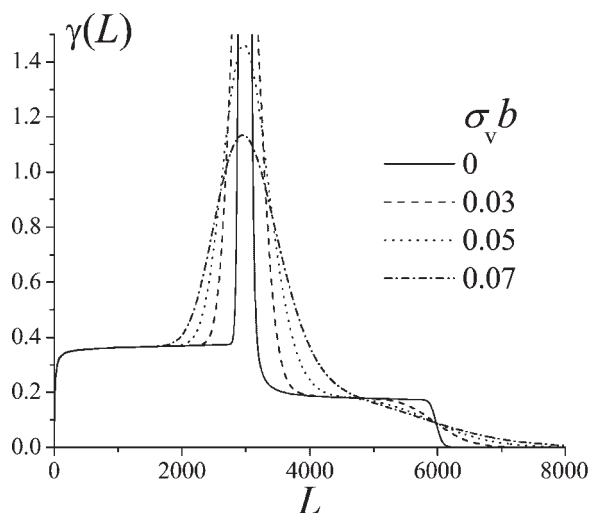


Figure 3. MWDs calculated for PLP of MMA at 25 °C and the high termination rate limit for different values of  $\sigma_v b$ . The kinetic parameters used for the simulation are:  $[M] = 9.354 \text{ mol} \cdot \text{L}^{-1}$ ,  $k_t = 4.1 \times 10^7 \text{ L} \cdot \text{mol}^{-1} \cdot \text{s}^{-1}$ ,  $k_p = 318 \text{ L} \cdot \text{mol}^{-1} \cdot \text{s}^{-1}$ ,  $\delta = 0.5$ ,  $C_M = 10^{-5}$ ,  $t_0 = 1 \text{ s}$ , and  $R_0 = 10^{-5} \text{ mol} \cdot \text{L}^{-1}$ .

different values of  $\sigma_v b$ , the dispersion parameter for SEC broadening. In the absence of broadening ( $\sigma_v b = 0$ ) the wide regions of distribution on the left and right sides from the peak are well described by Equation (12) and (15). For this particular simulation, these regions of distribution are parallel to the abscissa, as MWDs are calculated using the classical model with no chain-length dependencies [ $\alpha = 0$ ,  $\beta = 0$ ,  $p(L) = 1$ ,  $d(L) = 1$ ,  $\gamma_{\text{left}}(L) = \text{const} = \frac{a_p U}{2k_0} = h_1$ , and  $\gamma_{\text{right}}(L) = \frac{1}{2} \gamma_{\text{left}}(L) = h_2$ ]. Increasing the dispersion parameter strongly narrows these regions parallel to the abscissa, especially on the right side of the peak; for  $\sigma_v b = 0.03$  the region is still present on the right side but it disappears for  $\sigma_v b = 0.05$ . At first sight, this is a strong restriction for determining the value of  $h_2$  from the distribution. Nevertheless, it is possible to overcome this difficulty, as described below.

The SEC dispersion causes two main changes in the shape of the distribution (Figure 3), broadening the main peak located at chain length  $L_0 = k_p[M]t_0$ , and softening the sharp decrease in distribution at chain lengths  $2L_0$ . Although not parallel to the abscissa, the distributions calculated for  $\sigma_v b = 0.05$  and  $0.07$  in Figure 3 all pass through  $h_2$  at the same chain length on the right side of the peak; this point is the most robust value of  $L_2$  to determine the value of  $h_2$  required to estimate  $\delta$  by Equation (16). Three approaches have been considered to find  $L_2$ . Firstly, the arithmetic mean between  $L_0 = k_p[M]t_0$  and  $2L_0$  is taken ( $L_2 = 1.5L_0$ ); however, this approach does not give satisfactory results as it does not take into account the fact that the SEC broadening acts in the  $\log L$  scale. Thus, the second approach is to average between  $L_0$  and  $2L_0$  on the logarithmic scale such that  $L_2 = \sqrt{2}L_0$ . However, even this

approach does not take into account that the SEC broadening effect is stronger at the  $L_0$  peak than in the region at  $2L_0$ . An examination of the simulation results in Figure 3 indicates that a robust estimate for  $L_2$  is the chain length corresponding to the inflection point on the high MW side of the peak ( $L_{2\text{max}}$ ), determined by differentiating the distribution.

Note that for “normal” PLP experiments conducted away from the high termination rate limit, the second peak in the derivative plot is expected at chain length  $2L_0$ .<sup>[15]</sup> Sarnecki and Schweer<sup>[16]</sup> have discovered that at the high termination rate limit  $L_{2\text{max}}$  is close to  $1.5L_0$ . Our calculations show that  $L_{2\text{max}}$  depends on the value of  $\sigma_v b$ : in the absence of SEC broadening  $L_{2\text{max}}$  is close to  $2L_0$ ; it decreases to a minimum value close to  $1.5L_0$  as  $\sigma_v b$  is increased to approximately 0.04, and then increases slightly as  $\sigma_v b$  increases further. What is important is that through these shifts,  $L_{2\text{max}}$  provides a robust estimate of  $L_2$  for determining  $h_2$  for the estimation of  $\delta$ , as shown in Figure 4. For current SEC instrumentation, the value of  $\sigma_v b$  is expected to be in the region of 0.04–0.05.<sup>[27,41]</sup> Figure 4 shows that the recommended procedure for evaluating  $h_2$  is satisfactory for  $\sigma_v b \leq 0.06$ . Therefore, SEC broadening is not an obstacle for the application of the new method for determining  $\delta$ .

### Influence of $p(L)$ and $d(L)$ Functions

Current knowledge of MMA propagation and termination mechanisms at 25 °C can be used to estimate the  $p(L)$  and

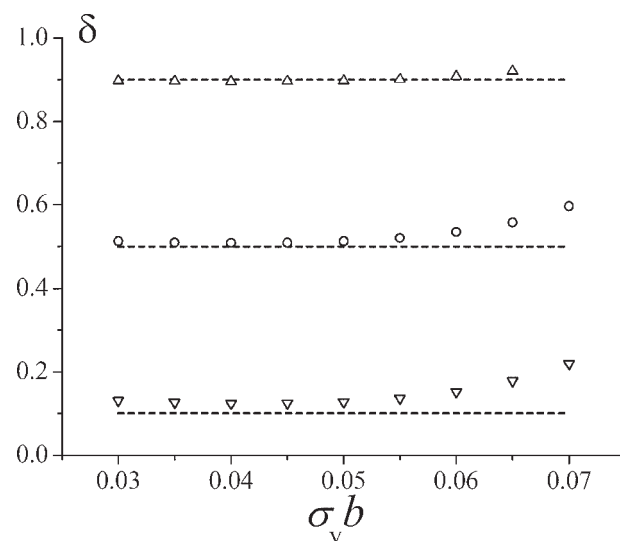
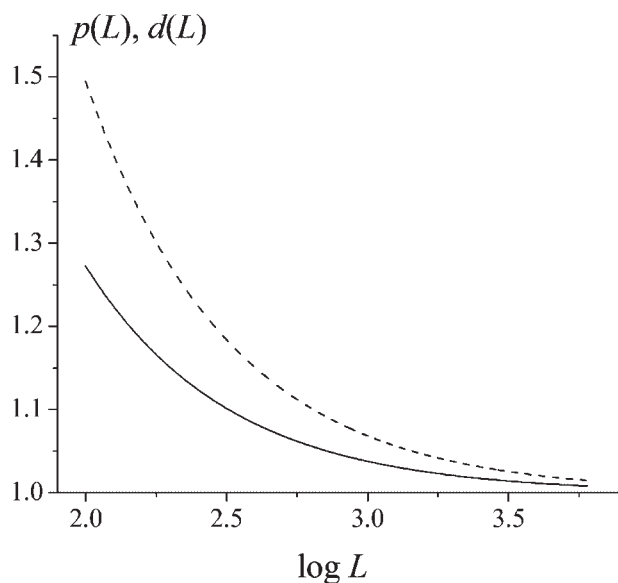


Figure 4. The values of  $\delta$  determined from numerical experiments with different values of  $\sigma_v b$ . The MWDs are calculated for PLP of MMA at 25 °C and the high termination rate limit:  $[M] = 9.354 \text{ mol} \cdot \text{L}^{-1}$ ,  $k_t = 4.1 \times 10^7 \text{ L} \cdot \text{mol}^{-1} \cdot \text{s}^{-1}$ ,  $k_p = 318 \text{ L} \cdot \text{mol}^{-1} \cdot \text{s}^{-1}$ ,  $C_M = 10^{-5}$ ,  $t_0 = 1 \text{ s}$ , and  $R_0 = 10^{-5} \text{ mol} \cdot \text{L}^{-1}$ . The input values of  $\delta = 0.1, 0.5$ , and  $0.9$  are shown by dashed lines. The output values of  $\delta$  are shown by “ $\nabla$ ” for the input value 0.1, by “ $\circ$ ” for the input value 0.5 and by “ $\Delta$ ” for the input value 0.9.

$d(L)$  functions defined by Equation (10). Recall that these functions capture the influence of stronger chain-length dependencies that occur at short chain lengths. For termination, the boundary chain length  $L_f$  is chosen as 100 and the power-law exponent  $e_1$  in Equation (7a) is set to 0.5.<sup>[30,34,36]</sup> For propagation, the critical chain length is known to be much smaller.<sup>[31]</sup> As presented in Appendix B, a value between chain lengths 7 and 8 can be estimated. Appendix B also presents other parameters required for evaluating  $p(L)$  and  $d(L)$  and the procedure for estimating  $b$  defined by Equation (10c); this latter value is determined to be  $1.24 \times 10^6 \text{ L} \cdot \text{mol}^{-1}$ . The resulting  $p(L)$  and  $d(L)$  functions, calculated according to Equation (10a) and (10b), are presented in Figure 5. As might be expected, the influence of the stronger propagation and termination chain-length dependencies for short chains on the resulting MWD is most evident (higher values of  $p$  and  $d$ ) at chain lengths closest to  $L_f (=100)$ , and becomes smaller with increasing chain lengths. For the experimental results discussed later, chain lengths above 1300 ( $\log L = 3.11$ ) are used to estimate kinetic parameters. At these chain lengths,  $p$  and  $d$  deviate from unity by less than 5%, and also do not vary greatly with  $L$ . While this small deviation might be ignored, we will consider its influence when estimating kinetic parameters from the experimental MWD.

The  $p(L)$  and  $d(L)$  functions are required as the chain-length laws for both propagation and termination deviate from Equation (6) for  $L \leq L_f$ . The values calculated in Figure 5 are based upon current understanding of these dependencies for MMA polymerization. It is interesting to



**Figure 5.** The  $p(L)$  (solid curve) and  $d(L)$  (dashed curve) functions for MMA polymerization at 25 °C. The following parameters are used for the calculation of these functions:  $\alpha = 0.07$ ,  $\beta = 0.21$ ,  $[M] = 9.354 \text{ mol} \cdot \text{L}^{-1}$ ,  $k_p^0 = 492 \text{ L} \cdot \text{mol}^{-1} \cdot \text{s}^{-1}$ ,  $k_t^0 = 5.85 \times 10^7 \text{ L} \cdot \text{mol}^{-1} \cdot \text{s}^{-1}$ ,  $L_f = 100$ , and  $b = 1.24 \times 10^6 \text{ L} \cdot \text{mol}^{-1}$ .

examine the behavior of these functions under limiting cases. First, consider the situation for which only the chain-length dependence for termination changes at  $L_f$  according to the composite model, while the power-law for propagation [Equation (6a)] is the same for all chain lengths  $L > 0$ . The resulting  $p(L)$  function is shown as curve 1 in Figure 6. The opposite extreme, for which the chain-length dependence for propagation changes at  $L_f$  (chosen to be 7–8, as discussed in Appendix B) while Equation (6b) for termination is the same for all chain lengths  $L > 0$ , is given by curve 3 in Figure 6. The two extremes examined have a considerable effect on the resulting  $p(L)$  function for  $L < 1000$ , with the assumption regarding the termination chain-length dependence (curve 3) having the largest effect on the shape and magnitude of the function. It is interesting to note the opposing influence of strong chain-length dependencies of propagation and termination for  $L < 1000$ . It is also important to note that, even for these two extremes, the values of  $p(L)$  are within a narrow range (0.99–1.07) for  $L > 1300$ . Thus, incomplete knowledge of the termination and propagation behavior of very short chains will not greatly effect the estimation of  $\delta$  from pMMA MWDs generated by PLP at the high termination rate limit.

The influence of  $p(L)$  and  $d(L)$  on the MWD is captured by the power-law exponent,  $\alpha_{\text{add}}$ , in Equation (13) and (14).

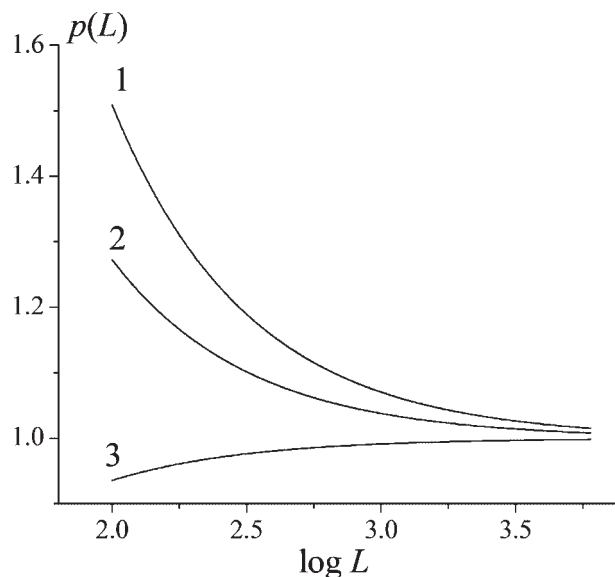


**Figure 6.** The  $p(L)$  functions calculated using (a) the composite model for termination and Equation (6a) for propagation for all chain lengths  $L > 0$  (curve 1); (b) Equation (6b) for termination for all chain lengths  $L > 0$  and the composite model for propagation (curve 3); (c) the composite models for both termination and propagation (curve 2). The following parameters are used for calculation of these functions:  $\alpha = 0.07$ ,  $\beta = 0.21$ ,  $[M] = 9.354 \text{ mol} \cdot \text{L}^{-1}$ ,  $k_p^0 = 492 \text{ L} \cdot \text{mol}^{-1} \cdot \text{s}^{-1}$ ,  $k_t^0 = 5.85 \times 10^7 \text{ L} \cdot \text{mol}^{-1} \cdot \text{s}^{-1}$ ,  $L_f = 100$ , and  $b = 1.24 \times 10^6 \text{ L} \cdot \text{mol}^{-1}$ .



Defining  $F(L) = \frac{\delta}{p(L)^2} + \frac{(1-\delta)2^{\alpha-\beta}}{d(L)^2}$  from Equation (14),  $\alpha_{\text{add}}$  can be estimated according to

$$\alpha_{\text{add}} = \frac{\ln[F(L+1)] - \ln[F(L)]}{\ln(L+1) - \ln(L)} \quad (17)$$

Values of  $\alpha_{\text{add}}$  are calculated in Figure 7 as a function of chain length for different values of  $\delta$ . For short chain lengths ( $L < 1000$ ),  $\alpha_{\text{add}}$  is strongly dependent on chain length, and varies significantly depending on whether termination is exclusively by disproportionation ( $\alpha_{\text{add}} \approx 0.37$  at  $L = 100$ ) or by combination ( $\alpha_{\text{add}} \approx 0.57$  at  $L = 100$ ). Fortunately,  $\alpha_{\text{add}}$  converges to a value relatively independent of chain length and mode of termination for longer chains. However, even for the interval  $1000 \leq L \leq 2000$  examined experimentally below, the value of  $\alpha_{\text{add}}$  ( $\approx 0.05$ ) is significantly greater than zero, and should be taken into account in the treatment of experimental data.

It is interesting that some evidence of the importance of  $\alpha_{\text{add}}$  can be deduced from literature. Olaj et al.<sup>[38]</sup> have estimated a value of 0.2 for  $\beta$  from a PMMA MWD produced at 25 °C by PLP at the high termination rate limit. This value was estimated using Equation (11), neglecting the influence of chain-length dependent propagation and the stronger dependencies occurring for short chain lengths. According to Equation (13), the value of 0.2 is actually an estimate of  $(\beta - \alpha + \alpha_{\text{add}})$ . In other works using different methodologies, Olaj et al.<sup>[25,43]</sup> have estimated  $(\beta - \alpha)$  for the same system to be 0.16–0.17. (This value is

reported as an estimate of  $\beta$ , as chain-length dependent propagation is not considered.) The difference of 0.03–0.04 is an indirect estimate for  $\alpha_{\text{add}}$ , and is close to the value of 0.05 estimated from Figure 7. It is interesting to note that Olaj et al.<sup>[38]</sup> observed a slight chain-length dependence for  $\beta$ , with the value increasing as chain length decreased; this finding is also in agreement with the increase in  $\alpha_{\text{add}}$  with decreasing  $L$  shown in Figure 7.

### Choice of Experimental Polymerization Conditions

Sarnecki and Schweer<sup>[16]</sup> were able to approach high termination rate limit conditions for MMA at 25 °C using a pulse frequency of 10 Hz. The fraction of radicals terminated between two successive laser pulses,  $\gamma_r$ , is calculated by Equation (3) to be very close to unity provided that the initial radical concentration,  $R_0$ , is of the order of  $10^{-5} \text{ mol} \cdot \text{L}^{-1}$ . Increasing the pulse separation time  $t_0$  further to 1 s (pulse frequency of 1 Hz) allows a high termination rate limit to be achieved at lower values of  $R_0$ . To illustrate this point, MWDs have been calculated for different modes of termination ( $\delta_{\text{input}} = 0.1, 0.5, 0.9$ ) as a function of  $R_0$  using the same model (no chain-length dependencies) as used for Figure 3 and 4. The output values of  $\delta$ , determined from these MWDs according to the procedures developed in this work, are presented in Figure 8. Satisfactory output values of  $\delta$  are obtained for  $R_0$  above  $2 \times 10^{-6} \text{ mol} \cdot \text{L}^{-1}$ , indicating that the high

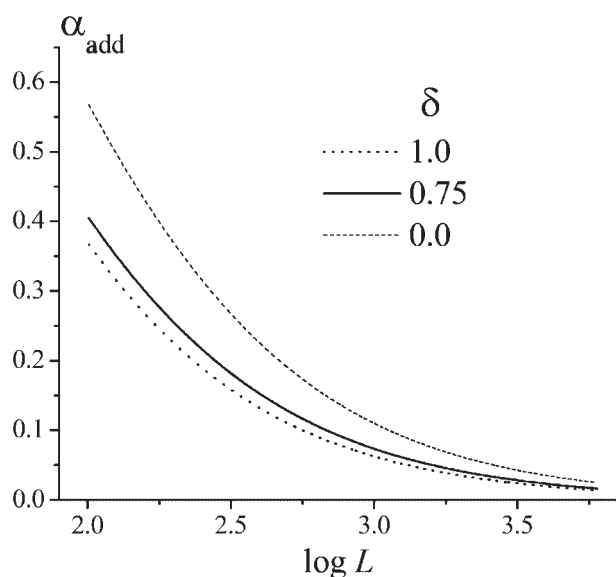


**Figure 7.** The values of  $\alpha_{\text{add}}$  calculated using Equation (17) for different values of  $\delta$ . The following parameters are used for calculation:  $\alpha = 0.07$ ,  $\beta = 0.21$ ,  $[M] = 9.354 \text{ mol} \cdot \text{L}^{-1}$ ,  $k_p^0 = 492 \text{ L} \cdot \text{mol}^{-1} \cdot \text{s}^{-1}$ ,  $k_t^0 = 5.85 \times 10^7 \text{ L} \cdot \text{mol}^{-1} \cdot \text{s}^{-1}$ ,  $L_f = 100$ , and  $b = 1.24 \times 10^6 \text{ L} \cdot \text{mol}^{-1}$ .

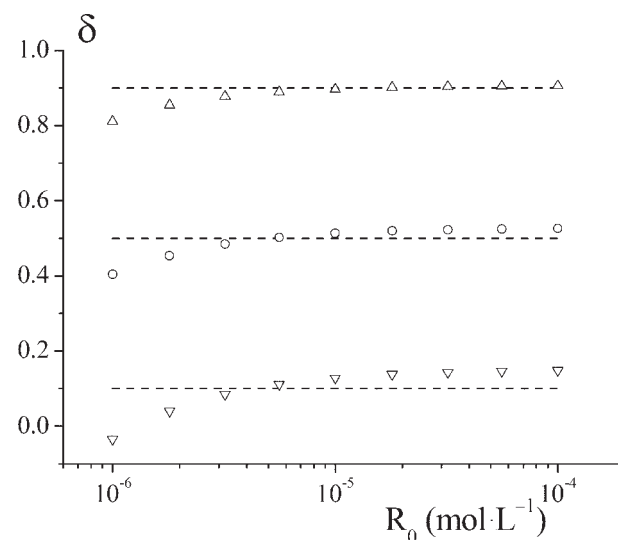


**Figure 8.** The values of  $\delta$  determined from numerical experiments with different values of  $R_0$ . MWDs are calculated for PLP of MMA at 25 °C and the high termination limit:  $[M] = 9.354 \text{ mol} \cdot \text{L}^{-1}$ ,  $k_t = 4.1 \times 10^7 \text{ L} \cdot \text{mol}^{-1} \cdot \text{s}^{-1}$ ,  $k_p = 318 \text{ L} \cdot \text{mol}^{-1} \cdot \text{s}^{-1}$ ,  $C_M = 10^{-5}$ ,  $\sigma_v b = 0.05$ , and  $t_0 = 1 \text{ s}$ . The input values of  $\delta = 0.1, 0.5$ , and  $0.9$  are shown by dashed lines. The output values of  $\delta$  are shown by “ $\nabla$ ” for the input value 0.1, by “o” for the input value 0.5 and by “ $\Delta$ ” for the input value 0.9.

termination rate limit can be easily achieved at reasonable values of  $R_0$ . The accuracy is slightly improved for the case of termination by disproportionation, showing that the method is well suited to determine  $\delta$  for the MMA system.

## Experimental Part

MMA (Fluka, 99% purity) is distilled under reduced pressure in the presence of dry  $K_2CO_3$  to remove the inhibitor (hydroquinone monomethyl ether) and is treated by several freeze and thaw cycles to remove dissolved oxygen. Darocur 1173 (2-hydroxy-2, 2-dimethylacetophenone, Merck) is added to the monomer at a concentration of  $10 \text{ mmol} \cdot \text{L}^{-1}$  under an argon atmosphere, and the mixture is transferred to an optical cell with a path length of 10 mm. The sample is maintained at  $25^\circ\text{C}$  while being exposed to pulsed laser radiation for 3 min (180 pulses at 1 Hz and an energy of 20 mJ per pulse) to allow for about 0.5% monomer conversion to polymer; the excimer laser (Lambda Physics) of 20 ns pulse width was operated on the XeF line at 351 nm. An inhibitor was added to prevent further polymerization after pulsing, and polymer was precipitated with an excess of methanol (analytical grade Fluka A6). The SEC analyses were performed at  $30^\circ\text{C}$  with tetrahydrofuran as the eluent on a system composed of a Waters pump (Model 515 HPLC), three PSS SDV ( $10^5$ ,  $10^3$ , and  $10^2 \text{ \AA}$ ) columns, and a Waters refractometer (Model 2410). Molecular weight analysis of the PMMA samples was carried out via calibration curves obtained with narrow PMMA standards.

## Results and Discussion

To achieve high termination rate conditions, attention should be paid to correct choice of the laser pulse energy, number of pulses, type of initiator and its concentration. Laser power absorption in the solution can lead to a spatial gradient in radical concentration, and initiator consumption during the sequence of pulses will cause  $R_0$  to vary with time.<sup>[44]</sup> Figure 8 indicates that it is necessary to have  $R_0$  greater than  $2 \times 10^{-6} \text{ mol} \cdot \text{L}^{-1}$  in order to accurately estimate  $\delta$ . The model formulated by Castignolles et al.<sup>[44]</sup> has been used to calculate the range of  $R_0$  values that will occur under the chosen experimental conditions for 300 pulses through a cell with a path length of 10 mm. As shown in Figure 9,  $R_0$  is estimated to vary between  $4.5 \times 10^{-6}$  and  $1.0 \times 10^{-5} \text{ mol} \cdot \text{L}^{-1}$ , well above the minimum value required to accurately estimate  $\delta$ .

The experimental MWD in the form of  $\gamma(L)$  obtained from PLP experiment of MMA polymerization at  $25^\circ\text{C}$  is given in Figure 10(a). The distribution is used to evaluate kinetic parameters of termination following the procedure given above.

### Estimation of $\beta$

The straight-line region of the distribution [Figure 10(a)] immediately before the peak with chain lengths between

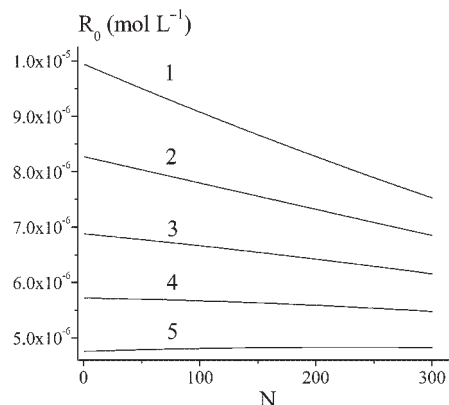


**Figure 9.** Initial radical concentrations produced by  $N^{\text{th}}$  laser pulse inside the  $i^{\text{th}}$  layer of solution using Darocur 1173 initiator with initial concentration of  $10 \text{ mmol} \cdot \text{L}^{-1}$  and laser pulse energy of 20 mJ. The solution is subdivided into five layers that are perpendicular to the direction of laser radiation, with layer 5 (curve 5) furthest removed from the incident light. The model and kinetic parameters used for calculation are given in ref.<sup>[44]</sup>

1 338 and 1 908 is used to estimate  $(\beta - \alpha + \alpha_{\text{add}})$  according to Equation (13) from a plot of  $\ln[\gamma(L)]$  versus  $\ln L$  [inset plot in Figure 10(a)]. Linear regression gives  $0.19 \pm 0.02$  for the slope, in excellent agreement with previous literature.<sup>[38]</sup> Estimating the value of  $\alpha_{\text{add}}$  as  $0.05 \pm 0.01$  from Figure 7 and taking  $\alpha = 0.07 \pm 0.02$  from previous literature,<sup>[26]</sup> a value of  $0.21 \pm 0.03$  is estimated for  $\beta$ . This value for the chain-length dependence of termination is very close to the original slope, as the influence of chain-length dependent propagation ( $\alpha$ ) and stronger chain-length dependencies of short chains ( $\alpha_{\text{add}}$ ) fortuitously cancel.

### Evaluation of $\delta$

Chain length  $L_1$  is chosen as the point closest to the peak on the linear fitted curve on the log-log plot shown in Figure 10(a):  $h_1 = 26.9$  at  $L_1 = 1\,886$ . (The estimate of  $\delta$  is not sensitive to the exact choice of  $L_1$ .) Chain length  $L_2$  is taken as the maximum of the second peak on the derivative plot shown as Figure 10(b):  $h_2 = 7.46$  at  $L_2 = 5\,402$ . To estimate  $\delta$  using Equation (16), the following values are evaluated using Equation (10) (see Figure 5):  $p(L_1) = 1.022$ ,  $d(L_1) = 1.040$  and  $d(L_2) = 1.016$ . With  $(\beta - \alpha) = 0.14$ , Equation (16a) is used to estimate the fraction of termination by disproportionation,  $\delta$ , as  $0.75 \pm 0.04$ . Application of Equation (16b) (neglecting chain-length dependencies of termination and propagation) yields  $\delta = 0.723$  with a difference of less than 4%. Thus, the methodology can be used to estimate  $\delta$  even if knowledge regarding chain-length dependent kinetics is lacking.

This estimate of 0.75 for  $\delta$  agrees well with estimates from other literature about the mode of termination

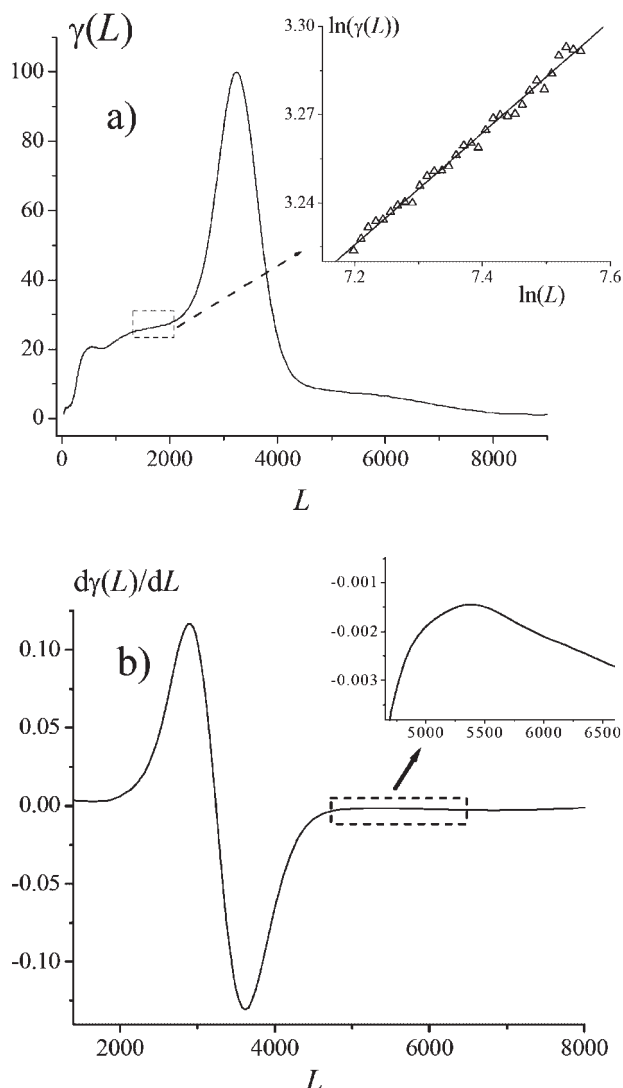


**Figure 10.** Experimental MWD (a) and associated first derivative (b) for PLP at high termination rate limit of MMA at 20 °C. Individual laser pulse energy and pulse separation were 20 mJ and 1 s, respectively. Photoinitiator (Darocur 1173) concentration was 10 mmol · L<sup>-1</sup> (see text for further experimental details).

for MMA,<sup>[5,6,9–11]</sup> including the estimate from Bevington et al.<sup>[7]</sup> of 0.69 determined using <sup>14</sup>C radiolabeled initiator, and the value of 0.66 estimated by Bamford et al.<sup>[8]</sup> using a gelation technique. Thus, we show that it is possible to obtain a reasonable measure of the mode of termination based upon analysis of MWDs produced by PLP, even when significant SEC broadening occurs, and even in the presence of chain-length dependent termination and combination.

## Conclusion

MWDs generated by PLP at the high termination rate limit provide valuable information about the nature of chain-

length dependent kinetics and the mode of termination. For MMA, the decrease in laser frequency to 1 Hz achieves this condition, provided that the concentration of radicals generated per pulse is above 10<sup>-6</sup> mol · L<sup>-1</sup>. MWDs produced at this high termination rate limit have several advantages. Firstly, the value of (β - α + α<sub>add</sub>) could be evaluated directly from the slope of the ln[γ(L)] versus lnL distribution. Secondly, the mode of termination could be evaluated according to a new method proposed here. The simulation for MMA polymerization at 25 °C confirms that the new method for estimating the mode of termination could be successfully applied in the presence of chain transfer to monomer and SEC broadening, and that the accuracy is reasonable even if chain-length dependencies are ignored while examining the experimental data. Application of the methodology to an experimental MWD obtained by PLP of MMA at 25 °C results in the following estimates: β = 0.21 ± 0.03 and δ = 0.75 ± 0.04. Experimental studies applying this new technique to other monomer systems are underway.

## Appendix A. Features of MWD at High Termination Rate Limit

Here, the explanation is given for the features of MWD obtained by PLP at the high termination rate limit. Consider the expression for the time dependence of the concentration of radicals produced by a laser pulse<sup>[33]</sup>

$$R(t) = \frac{R_0}{1 + R_0 \int_0^t k_t^{\psi(t'), \psi(t')} dt'} \quad (\text{A1})$$

It can be easily seen that for times  $t \geq t_p$ , where  $t_p$  follows the condition

$$R_0 \int_0^{t_p} k_t^{\psi(t'), \psi(t')} dt' \gg 1 \quad (\text{A2})$$

the remaining concentration of radicals is much less than the initial concentration:  $R(t) \ll R_0$  (in addition, the remaining concentration does not depend on the value of  $R_0$ :  $R(t) \approx \left[ \int_0^t k_t^{\psi(t'), \psi(t')} dt' \right]^{-1}$ ). Then by choosing a pulse separation time  $t_0 \geq t_p$  for PLP we come to the situation at which the concentration of radicals produced by a new pulse is much higher than the concentration of radicals remaining from the former pulse. According to Equation (A2), higher values of  $R_0$  result in lower values of  $t_p$

such that a smaller pulse separation time is required to achieve the high termination rate limit. Increased  $R_0$  also leads to the faster termination between “old” (those generated at the previous pulse) and “new” radicals. These termination events have negligible effect on the concentration of new radicals in the system, as this concentration is much higher than the concentration of surviving radicals from the previous pulse. Therefore, the polymerization of radicals produced by a new pulse is well approximated by single pulse polymerization.

The radicals produced by each pulse pass through two stages during polymerization at the high termination rate limit. In the first stage, immediately after production, they have a status of new radicals, and their polymerization can be described in terms of a single pulse polymerization, as described by Equation (4). At time  $t_0$  the surviving radicals become old and are terminated immediately by reaction with the high concentration of radicals generated by the next pulse. This termination leads to the appearance of a sharp peak in the  $w(\log M)$  form of the MWD. Thus, there are two contributions to the overall MWD: the first from the single pulse polymerization by mutual termination of new radicals and the second the peak formed due to the instantaneous “new–old” termination that occurs at  $t_0$ .

The peak resulting from new–old termination is located approximately at chain length  $\psi(t_0)$ , independent of the mode of termination. At the same time, the MWD resulting from “new–new” termination is described by Equation (4). This will occur in the chain length region  $0 < L \leq 2\psi(t_0)$  for the case of termination exclusively by combination [as the termination of radicals having chain length  $\psi(t)$  leads to the formation of a macromolecule having chain length  $2\psi(t)$ ], and within the chain length region  $0 < L \leq \psi(t_0)$  in the case of termination exclusively by disproportionation. Thus, only termination by combination contributes to the distribution on the right (high MW) side of the main peak.

The fulfillment of condition A2 simplifies the expression for MWDs at chain lengths close to  $\psi(t_0)$ ; i.e., at the vicinity of the PLP peak. According to Equation (4), the following expression could be written for the distribution at these chain lengths

$$n_s(L) = \frac{k_{td}^{L,L}}{2[M]k_p^L \left( \int_0^{\psi(L)} k_t^{\psi(t'), \psi(t')} dt' \right)^2} + \frac{k_{tc}^{L/2, L/2}}{8[M]k_p^{L/2} \left( \int_0^{\psi(L/2)} k_t^{\psi(t'), \psi(t')} dt' \right)^2} \quad (A3)$$

Using the power-law representation of propagation and termination, Equation (A3) becomes

$$n_s(L) = \frac{(1 + \alpha - \beta)^2 UL^{\beta - \alpha - 2}}{2k_t^0} \left( \frac{\delta}{p(L)^2} + \frac{(1 - \delta)2^{\alpha - \beta}}{d(L)^2} \right) \quad (A4)$$

## Appendix B. Estimation of $b$ Value

The region of chain length up to the value of  $L_f$  is subdivided into two regions. In the first region propagation is chosen to obey Equation (8)<sup>[31]</sup> with  $C_1 = 15.8$ ,  $i_{1/2} = 1.12$ , and with the long-chain propagation rate coefficient  $k_p$  chosen to be equal to the value recommended by IUPAC.<sup>[40]</sup> In the second region, propagation is chosen to obey Equation (6a) with  $\alpha = 0.07$ ,<sup>[26]</sup> and  $k_p^0 = 492 \text{ L} \cdot \text{mol}^{-1} \cdot \text{s}^{-1}$  to give a satisfactory reproduction of experiments from ref.<sup>[29]</sup> The chain length  $L_c$  separating these two parts is found by the numerical solution of Equation (B1).

$$k_p \left[ 1 + C_1 \exp \left( -\frac{\ln 2}{i_{1/2}} (L_c - 1) \right) \right] - k_p^0 L_c^{-\alpha} = 0 \quad (B1)$$

This solution gives  $L_c$  to be between chain length 7 and 8 (the exact virtual value of  $L_c = 7.2$ ). The time  $t_c$  needed for radicals to grow up to value  $L_c$  is calculated according to

$$t_c = \frac{i_{1/2}}{\ln 2 [M] k_p} \ln \left[ \frac{C_1 \exp \left( \frac{\ln 2}{i_{1/2}} \right) \left( 1 + C_1 \exp \left( -\frac{\ln 2}{i_{1/2}} (L_c - 1) \right) \right)}{\left( 1 + C_1 \exp \left( \frac{\ln 2}{i_{1/2}} \right) \right) C_1 \exp \left( -\frac{\ln 2}{i_{1/2}} (L_c - 1) \right)} \right] \quad (B2)$$

Equation (B2) is found by integration of Equation (5) according to Equation (B3) for  $L = L_c$  and  $t = t_c$ .

$$\int_0^{L_c} \frac{dL'}{k_p^{L'}} = \int_0^{t_c} [M] dt' = [M] t_c \quad (B3)$$

Also Equation (B3) allows the prediction of how the chain length of growing radicals changes with time in the region  $0 \leq L \leq L_c$

$$L = 1 - \frac{i_{1/2}}{\ln 2} \ln \left[ \frac{y(t)}{(1 - y(t)) C_1} \right] \quad (B4a)$$

where

$$y(t) = \frac{C_1 \exp\left(\frac{\ln 2}{i_{1/2}}\right)}{1 + C_1 \exp\left(\frac{\ln 2}{i_{1/2}}\right)} \exp\left(-\frac{\ln 2}{i_{1/2}}[M]k_p t\right) \quad (\text{B4b})$$

In addition, the integration of Equation (B3) leads to the expression for time  $t_f$  that is required for radicals to increase to length  $L_f$

$$t_f = t_c + \frac{(L_f^{1+\alpha} - L_c^{1+\alpha})}{k_p^0[M](1+\alpha)} \quad (\text{B5})$$

The time dependence of radical chain length in the region  $L_c \leq L \leq L_f$  is given by

$$L = [L_c^{1+\alpha} + k_p^0[M](1+\alpha)(t - t_c)]^{\frac{1}{1+\alpha}} \quad (\text{B6})$$

The chain-length dependence of termination is taken into account according to the composite model [Equation (7a)]<sup>[30,34]</sup> with  $k_t^{1,1} = 2.8 \times 10^8 \text{ L} \cdot \text{mol}^{-1} \cdot \text{s}^{-1}$  and  $e_1 = 0.5$ . The value  $k_t^{1,1} = 2.8 \times 10^8$  is chosen to give  $k_t^0 = 5.85 \times 10^7 \text{ L} \cdot \text{mol}^{-1} \cdot \text{s}^{-1}$  for Equation (6b), in agreement with experimental data in ref.<sup>[43]</sup> Then the following mathematical transformations from Equation (10c) could be made for the calculation of  $b$  using Equation (B2) and (B4)–(B6).

$$\begin{aligned} b &= \int_0^{\psi(L_f)} k_t^{\psi(t'), \psi(t')} dt' \\ &= \int_0^{t_c} k_t^{\psi(t'), \psi(t')} dt' + \int_{t_c}^{t_f} k_t^{\psi(t'), \psi(t')} dt' \\ &= k_t^{1,1} \int_0^{t_c} \left[ 1 - \frac{i_{1/2}}{\ln 2} \ln \left( \frac{y(t')}{(1 - y(t'))C_1} \right) \right]^{-e_1} \\ &\quad \times dt' + \frac{k_t^{1,1}(L_f^{1+\alpha-e_1} - L_c^{1+\alpha-e_1})}{k_p^0[M](1+\alpha-e_1)} \end{aligned} \quad (\text{B7})$$

**Acknowledgements:** We thank Professor Michael Buback for helpful discussions and access to laboratory facilities.

Received: August 28, 2006; Revised: November 3, 2006; Accepted: November 6, 2006; DOI: 10.1002/mats.200600061

**Keywords:** free radical polymerization; mechanistic model; methyl methacrylate; mode of termination; molecular-weight

distribution/molar mass; pulsed laser polymerization; radical polymerization; termination kinetics

- [1] M. Buback, H. Hippler, J. Schweer, H.-P. Vögele, *Makromol. Chem. Rapid Commun.* **1986**, *7*, 261.
- [2] S. Beuermann, M. Buback, *Prog. Polym. Sci.* **2002**, *27*, 191.
- [3] C. H. Bamford, W. G. Barb, A. D. Jenkins, P. F. Onyon, "The Kinetics of Vinyl Polymerization by Radical Mechanism", Butterworths, London 1958.
- [4] H. S. Bagdasarian, "The Theory of Radical Polymerization" (in Russian), Nauka, Moscow 1966.
- [5] G. C. Eastmond, "Comprehensive Chemical Kinetics", C. H. Bamford, C. F. H. Tipper, Eds., Elsevier, Amsterdam 1976, Vol. 14 A., p. 61.
- [6] G. Moad, D. H. Solomon, "The Chemistry of Free Radical Polymerization", Elsevier, Oxford 1995.
- [7] J. C. Bevington, H. W. Melville, R. P. Taylor, *J. Polym. Sci.* **1954**, *12*, 449.
- [8] C. H. Bamford, R. W. Dyson, G. C. Eastmond, *J. Polym. Sci. Part C* **1967**, *16*, 2425.
- [9] M. D. Zammit, T. P. Davis, D. M. Haddleton, K. G. Suddaby, *Macromolecules* **1997**, *30*, 1915.
- [10] M. J. Gibian, R. C. Corley, *Chem. Rev.* **1973**, *73*, 441.
- [11] Z. B. Alfassi, "Chemical Kinetics of Small Organic Radicals", Z. B. Alfassi, Ed., CRS Press, Boca Raton 1988, Vol. 1, Chapter 6.
- [12] O. F. Olaj, I. Bitai, F. Hinkelmann, *Makromol. Chem.* **1987**, *188*, 1689.
- [13] O. F. Olaj, I. Schnöll-Bitai, *Eur. Polym. J.* **1989**, *25*, 635.
- [14] M. Buback, M. Egorov, R. G. Gilbert, V. Kaminsky, O. F. Olaj, G. T. Russell, P. Vana, G. Zifferer, *Macromol. Chem. Phys.* **2002**, *203*, 2570.
- [15] S. Beuermann, D. A. Paquet, J. H. McMinn, R. A. Hutchinson, *Macromolecules* **1996**, *29*, 4206.
- [16] J. Sarnecki, J. Schweer, *Macromolecules* **1995**, *28*, 4080.
- [17] M. L. Coote, M. D. Zammit, T. P. Davis, *Trends Polym. Sci.* **1996**, *4*, 189.
- [18] A. M. van Herk, *Macromol. Theory Simul.* **2000**, *9*, 433.
- [19] R. A. Hutchinson, D. A. Paquet, J. H. McMinn, *Macromolecules* **1995**, *28*, 5655.
- [20] M. Buback, R. A. Lämmel, *Macromol. Theory Simul.* **1997**, *6*, 145.
- [21] A. N. Nikitin, A. V. Evseev, *Chem. Phys. (Russia)* **2002**, *21*, 50.
- [22] M. Deady, A. W. H. Mau, G. Moad, T. H. Spurling, *Macromol. Chem. Phys.* **1993**, *194*, 1691.
- [23] A. N. Nikitin, A. V. Evseev, *Macromol. Theory Simul.* **1999**, *8*, 296.
- [24] O. F. Olaj, P. Vana, M. Zoder, A. Kornherr, G. Zifferer, *Macromol. Rapid Commun.* **2000**, *21*, 913.
- [25] O. F. Olaj, A. Kornherr, G. Zifferer, *Macromol. Theory Simul.* **2001**, *10*, 881.
- [26] A. N. Nikitin, A. V. Evseev, M. Buback, A. Feldermann, M. Jürgens, D. Nelke, *Macromol. Theory Simul.* **2002**, *11*, 961.
- [27] S. Beuermann, *Macromolecules* **2002**, *35*, 9300.
- [28] R. X. E. Willemsse, B. B. Staal, A. M. van Herk, S. C. J. Pierik, B. Klumperman, *Macromolecules* **2003**, *36*, 9797.
- [29] O. F. Olaj, M. Zoder, P. Vana, A. Kornherr, I. Schnöll-Bitai, G. Zifferer, *Macromolecules* **2005**, *38*, 1944.
- [30] G. B. Smith, G. T. Russell, M. Yin, J. P. A. Heuts, *Eur. Polym. J.* **2005**, *41*, 225.
- [31] J. P. A. Heuts, G. T. Russell, *Eur. Polym. J.* **2006**, *42*, 3.



- [32] A. V. Evseev, A. N. Nikitin, *Proc. SPIE* **1996**, 2713, 381.
- [33] A. N. Nikitin, *Polym. Sci., Ser. A* **2003**, 45, 847.
- [34] G. B. Smith, J. P. A. Heuts, G. T. Russell, *Macromol. Symp.* **2005**, 226, 133.
- [35] A. N. Nikitin, A. V. Evseev, "Pseudo-single-pulse Polymerization as a Tool of Investigation of Chain Length Dependence of Termination Constant", in: *A Lecture Presented at the World Polymer Congress -Macro98*, Gold Coast, Australia, 12–17 July, 1998.
- [36] G. B. Smith, G. T. Russell, J. P. A. Heuts, *Macromol. Theory Simul.* **2003**, 12, 299.
- [37] A. N. Nikitin, A. V. Evseev, *Macromol. Theory Simul.* **1997**, 6, 1191.
- [38] O. F. Olaj, P. Vana, A. Kornherr, G. Zifferer, *Macromol. Chem. Phys.* **1999**, 200, 2031.
- [39] A. N. Nikitin, P. Castignolles, B. Charleux, J.-P. Vairon, *Macromol. Theory Simul.* **2003**, 12, 440.
- [40] S. Beuermann, M. Buback, T. P. Davis, R. G. Gilbert, R. A. Hutchinson, O. F. Olaj, G. T. Russell, J. Schweer, A. M. van Herk, *Macromol. Chem. Phys.* **1997**, 198, 1545.
- [41] M. Buback, M. Busch, R. A. Lämmel, *Macromol. Theory Simul.* **1996**, 5, 845.
- [42] M. Stickler, G. Meyerhoff, *Makromol. Chem.* **1978**, 179, 2729.
- [43] O. F. Olaj, P. Vana, *Macromol. Rapid Commun.* **1998**, 19, 533.
- [44] P. Castignolles, A. N. Nikitin, L. Couvreur, G. Mouraret, B. Charleux, J.-P. Vairon, *Macromol. Chem. Phys.* **2006**, 207, 81.